Meccanica (2017) 52:1527–1539
DOI 10.1007/s11012-016-0517-9

# Active and passive controls of nanoparticles in Maxwell stagnation point flow over a slipped stretched surface

**N. A. Halim · Rizwan Ul Haq · N. F. M. Noor**

Received: 14 January 2016 / Accepted: 13 August 2016 / Published online: 19 August 2016


**Abstract** A steady stagnation-point flow of an incompressible Maxwell fluid towards a linearly stretching sheet with active and passive controls of nanoparticles is studied numerically. The momentum equation of the Maxwell nanofluid is inserted with an external velocity term as a result of the flow approaches the stagnation point. Conventional energy equation is modified by incorporation of nanofluid Brownian and thermophoresis effects. The condition of zero normal flux of nanoparticles at the stretching surface is defined to impulse the particles away from the surface in combination with nonzero normal flux condition. A hydrodynamic slip velocity is also added to the initial condition as a component of the entrenched stretching velocity. The governing partial differential equations are then reduced into a system of ordinary differential equations by using similarity transformation. A classical shooting method is applied to solve the nonlinear coupled differential equations. The velocity, temperature and nanoparticle volume fraction profiles together with the reduced skin friction coefficient, Nusselt number and Sherwood number are graphically presented to visualize the effects of particular parameters. Temperature distributions in passive control model are consistently lower than in the active control model. The magnitude of the reduced skin friction coefficient, Nusselt number and Sherwood number decrease as the hydrodynamic slip parameter increases while the Brownian parameter has negligible effect on the reduced heat transfer rate when nanoparticles are passively controlled at the surface. It is also found that the stagnation parameter contributes better heat transfer performance of the nanofluid under both active and passive controls of normal mass flux.

**Keywords** Stagnation point · Maxwell fluid · Zero flux · Hydrodynamic slip · Nanofluid · Boundary layer · Stretching

## 1 Introduction

Most of the working fluids at industrial level belong to non-Newtonian fluids. They are multi-component and chemically complex, and they display shear-dependence of viscosity, thixotropy and elasticity in different degrees [1]. Considerable efforts have been directed towards understanding the characteristics of these so-called rheological fluids because of their growing use in various manufacturing and processing industries. Some of the applications include hot rolling paper production, optical fibers, plastic polymers and

N. A. Halim · N. F. M. Noor (✉)
Institute of Mathematical Sciences, Faculty of Science, University of Malaya, 50603 Kuala Lumpur, Malaysia
e-mail: drfadiya@um.edu.my

R. U. Haq
Department of Mathematics, Quaid-i-Azam University, Islamabad 44000, Pakistan

many more. Several models have been proposed over the years in the attempt to explain behavior of the non-Newtonian fluids. One of the earliest models that gained much acceptance is the power-law model in which the shear stress varies according to a power function of the strain rate [2].

Schowalter [3] and Acrivos et al. [4] were the first to perform the theoretical analysis of a steady boundary layer flow of incompressible power-law fluids in 1960. Since then, more and better models have been proposed to suit different types of non-Newtonian behavior such as Jeffrey fluid, Bingham fluid, Oldroyd-B fluid and Casson fluid, to name a few. These fluids are generally categorized into rate-, differential- and integral-type fluids. Amongst the abundance of the non-Newtonian models, there is Maxwell model which is the simplest subclass of rate-type fluid that can predict the relaxation time effects. Investigations involving Maxwell fluid are plenty [5–9]. Some recent ones include the study by Hussain et al. [10] on the impact of double stratification and magnetic field in mixed convective radiative flow of Maxwell nanofluid. Their study showed that the thermal stratification parameter and concentration stratification parameter caused a reduction in temperature and nanoparticle concentration. Khan et al. [11] investigated the heat and mass transfer on MHD mixed convection axisymmetric chemically reactive flow of a Maxwell fluid driven by exothermal and isothermal stretching disks.

The stagnation point flow over a stretching surface is a classic problem in fluid mechanics. Hiemenz was the first to investigate the steady flow in the neighborhood of a stagnation point [12]. Various studies have been conducted since then to study the stagnation-point flows of many other Newtonian and non-Newtonian fluids [12–16]. The study on nanofluids is gaining much interest due to its capacity in improving thermal conductivity of regular fluids such as water, oil, ethylene glycol and synthetic oil. Mustafa et al. [17] are one of the first few who investigate the stagnation-point flow of a nanofluid. They take into account the combined effects of heat and mass transfer in the presence of Brownian motion and thermophoresis. Then, Bachok et al. [18] investigated the boundary layer of an unsteady two-dimensional stagnation-point flow of a nanofluid. Alsaedi et al. [19] further conducted an analysis to examine the stagnation point flow of nanofluid near a permeable stretched surface with a convective boundary condition. Noor et al. [20] investigated the mixed convection stagnation flow of a micropolar nanofluid along a vertically stretching surface with slip effects. Their findings show that the presence of slip velocity between the base fluid and the nanoparticles has significant impact on the heat transfer enhancement for the stagnation flow of micropolar nanofluid. Most recently, Ramesh et al. [21] have carried out an analysis to study the stagnation point flow of Maxwell fluid towards a permeable stretching sheet in the presence of nanoparticles. Their study showed increasing trend of velocity and decreasing temperature and concentration profile when the Maxwell parameter is increased.

Nield and Kuznetsov [22] made an assumption that one could control the value of the nanoparticle fraction at the boundary the same way one could control the temperature. However, no indication is given on how it could be done in practice. They recently revised the problem [23] by replacing the boundary condition with a more physically realistic set that accounts for the effect of both Brownian and thermophoresis parameters. It is now assumed that there is no normal mass flux at the plate and that the particle fraction value there adjusts accordingly. Since then, more models are presented by taking into consideration the zero normal flux of nanoparticles at the wall. Nield and Kuznetsov themselves have revised a few of their existing models on the corresponding problems in the onset of convection in a horizontal nanofluid layer of finite depth [24], in natural convective boundary layer flow of a nanofluid [25] and in a thermal instability analysis of a nanofluid-saturated porous layer [26]. Rahman et al. [27] investigated numerically the steady boundary layer flow and heat transfer characteristics of a nanofluid using Buongiorno's model past a permeable exponentially shrinking/stretching surface with second order slip velocity. Mustafa et al. [28] explored the boundary layer flow due to a convectively heated non-linearly stretching sheet. Haq et al. [29] discussed the combined effects of both thermal radiation and thermal slip on MHD boundary layer stagnation-point fluid flow along a porous surface which is saturated by nanoparticles. Their result shows that the thermal slip parameter decreases the

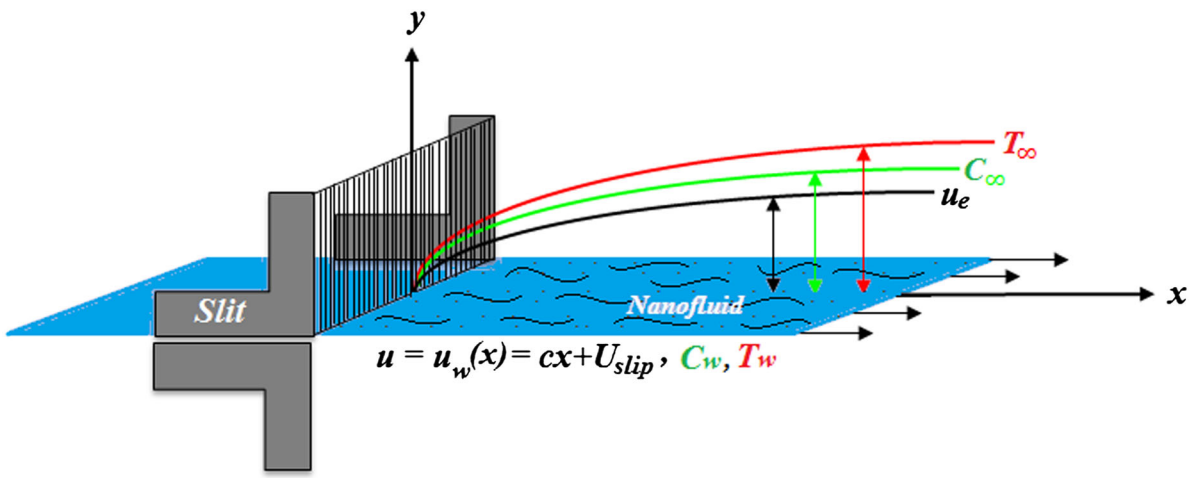


**Fig. 1** Diagram of the stagnation flow of Maxwell fluid saturated with nanoparticle

temperature profile while the radiation parameter increases the temperature profile. Zaimi et al. [30] investigated the problem of a nanofluid flow due to a permeable stretching/shrinking sheet while Dhanai et al. [31] investigated the combined effects of magnetic field and viscous dissipation in the mass transfer of a steady boundary layer nanofluid flow induced by a power law stretching/shrinking sheet.

Sadeghy et al. [32] opted to study the stagnation-point flow of viscoelastic fluids by relying on a more realistic constitutive equation. They proposed that upper-convected Maxwell (UCM) model is the best candidate to study the effects of fluid elasticity on the characteristics of its boundary layer in stagnation-point flow. To authors' best knowledge, studies with regard to stagnation-point flow of a Maxwell nanofluid are scarce. Moreover, the effects of hydrodynamic slip velocity combined with both zero and nonzero normal mass fluxes have been introduced into the model for the first time. The expression of passive control on nanoparticles was previously proposed by Kuznetsov and Nield [23] to investigate the passive control of normal mass flux on the flow characteristics towards a stretching surface. The present work used a similarity approach to reduce the nonlinear partial differential equations into a system of ordinary differential equation before they are solved numerically. The results obtained are then tabulated and shown graphically to illustrate the influence of various parameters on flow, heat and mass transfer characteristics.

## 2 Problem formulation

### 2.1 Governing equations and boundary conditions

Consider a 2-dimensional steady stagnation-point flow of an incompressible Maxwell fluid towards a horizontal linearly stretching sheet which coincides with the plane $y = 0$. The flow depicted in Fig. 1 is assumed to be confined to $y > 0$ with the stretching velocity $u_w(x) = cx$ while the velocity external to the boundary layer flow is $u_e(x) = ax$ where $a$ and $c$ are positive constants. Temperature at the surface of the wall is defined as $T_w$. Nanoparticle volume concentration takes the value $C_w$ at the surface for actively controlled mass flux while the ambient temperature and concentration are denoted by $T_\infty$ and $C_\infty$ respectively. The nanoparticle volume fraction for passively controlled mass flux is defined separately by the temperature gradient resulting with zero normal flux of nanoparticles.

By mean of the above said assumptions, the governing continuity, momentum, energy and concentration equations are defined as

$$\frac{\partial u}{\partial x} + \frac{\partial v}{\partial y} = 0, \tag{1}$$

$$u\frac{\partial u}{\partial x}+v\frac{\partial u}{\partial y}=u_e\frac{du_e}{dx}+\nu\frac{\partial^2 u}{\partial y^2} - k_1\left(u^2\frac{\partial^2 u}{\partial x^2}+v^2\frac{\partial^2 u}{\partial y^2}+2uv\frac{\partial^2 u}{\partial x\partial y}\right), \tag{2}$$

$$u\frac{\partial T}{\partial x}+v\frac{\partial T}{\partial y}=\kappa\frac{\partial^2 T}{\partial y^2}+\tau D_B\frac{\partial C}{\partial y}\frac{\partial T}{\partial y}+\frac{\tau D_T}{T_\infty}\left(\frac{\partial T}{\partial y}\right)^2, \tag{3}$$

$$u\frac{\partial C}{\partial x}+v\frac{\partial C}{\partial y}=D_B\frac{\partial^2 C}{\partial y^2}+\frac{D_T}{T_\infty}\frac{\partial^2 T}{\partial y^2}. \tag{4}$$

The Eq. (2) is proposed by Hayat et al. [12] in 2009 while the Eqs. (3) and (4) are initially introduced by Buongiorno [33] in 2006. In these equations, $u$ and $v$ are the velocity components in the $x$ and $y$ directions respectively, $\mu$ is the dynamic viscosity, $\nu$ is the kinematic viscosity, $k_1$ is the relaxation time of the UCM fluid, $\kappa$ is the thermal diffusivity, $D_B$ is the Brownian diffusion coefficient, $D_T$ is the thermophoretic diffusion coefficient and $\tau$ is the ratio of effective heat capacity between the nanoparticles material and the fluid. The boundary conditions for the flow are given as

$$u=u_w(x)=cx+U_{slip},\quad v=0,\quad T=T_w, \tag{5}$$

$$\begin{cases} D_B\dfrac{\partial C}{\partial y}+\dfrac{D_T}{T_\infty}\dfrac{\partial T}{\partial y}=0, & \text{(passive control of } \phi) \\ C=C_w, & \text{(active control of } \phi) \end{cases} \tag{6}$$

$$\begin{aligned} &\text{at}\quad y=0,\\ &u=u_e(x)=ax,\quad v=0,\quad T=T_\infty,\quad C=C_\infty\\ &\text{as}\quad y\to\infty, \end{aligned} \tag{7}$$

where the passive control condition that represents the normal mass flux is currently defined by Kuznetsov and Nield [23]. Finally, we introduce hydrodynamic slip velocity, $U_{slip}$ along the stretching surface in (5) which is defined as

$$U_{slip}=\alpha_w\left[(1+k_1c)\frac{\partial u}{\partial y}\right], \tag{8}$$

where $\alpha_w$ is the dimensional slip coefficient.

## 2.2 Similarity transformation

The governing Eqs. (2)–(4) can be transformed to a set of non-linear ordinary differential equations by introducing the following non-dimensional variables:

$$\eta=y\sqrt{\frac{c}{\nu}},\quad \psi=\sqrt{c\nu}xf(\eta),\quad \theta(\eta)=\frac{T-T_\infty}{T_w-T_\infty},$$
$$\begin{cases} \phi(\eta)=\dfrac{C-C_\infty}{C_\infty}, & \text{(passive control of } \phi) \\ \phi(\eta)=\dfrac{C-C_\infty}{C_w-C_\infty}, & \text{(active control of } \phi) \end{cases} \tag{9}$$

where $\psi$ is the stream function which satisfies (1) and

$$u=\frac{\partial\psi}{\partial y}=cxf'(\eta)\quad\text{and}\quad \mathrm{v}=-\frac{\partial\psi}{\partial \mathrm{x}}=-\sqrt{\nu c}\mathrm{f}(\eta). \tag{10}$$

Using the expressions (9) and (10), the nonlinear ordinary differential equations are obtained as

$$f'''-(f')^2+ff''+r^2+K(2ff'f''-f^2f''')=0, \tag{11}$$

$$\theta''+\mathrm{Pr}\left[f\theta'+Nb\,\theta'\phi'+Nt(\theta')^2\right]=0, \tag{12}$$

$$\phi''+Le\,\mathrm{Pr}f\phi'+\frac{Nt}{Nb}\theta''=0, \tag{13}$$

subject to the corresponding boundary conditions

$$f(0)=0,\quad f'(0)=1+\alpha(1+K)f''(0),\quad \theta(0)=1,$$
$$\begin{cases} Nb\phi'(0)+Nt\,\theta'(0)=0, & \text{(passive control of } \phi) \\ \phi(0)=1, & \text{(active control of } \phi) \end{cases} \tag{14}$$

$$f(\infty)=0,\quad f'(\infty)=r,\quad \theta(\infty)=0,\quad \phi(\infty)=0. \tag{15}$$

where primes denote differentiation with respect to $\eta$. Here, $r=a/c$ is the stagnation parameter, $K=k_1c$ is the elasticity parameter, $\mathrm{Pr}=\nu/\kappa$ is the Prandtl number, $Le=\kappa/D_B$ is the Lewis number and $\alpha=\alpha_w\sqrt{c/\nu}$ denotes the slip coefficient. The parameters of Brownian motion $Nb$ and thermophoresis $Nt$ are defined as

$$\begin{cases} Nb = \dfrac{\tau D_T C_\infty}{\nu}, & \text{(passive control of } \phi) \\ Nb = \dfrac{\tau D_T (C_w - C_\infty)}{\nu}, & \text{(active control of } \phi) \end{cases}$$
$$Nt = \frac{\tau D_T (T_w - T_\infty)}{\nu T_\infty}. \tag{16}$$

The physical quantities of interest are the local skin friction coefficient, the wall heat transfer coefficient (or the local Nusselt number) and the wall deposition flux (or the local Sherwood number). These expressions are defined as

$$Cf_x = \frac{\tau_w}{\rho\, u_w^2(x)}, \quad Nu_x = \frac{q_w x}{\kappa(T_w - T_\infty)}, \quad Sh_x = -\frac{q_m x}{D_B(C_w - C_\infty)}, \tag{17}$$

where the wall shear stress $\tau_w$, wall heat transfer $q_w$ and the wall mass flux $q_m$ are given by

$$\tau_w = \mu(1+K)\left(\frac{\partial u}{\partial y}\right)_{y=0}, \quad q_w = -\kappa\left(\frac{\partial T}{\partial y}\right)_{y=0}, \quad q_m = -D_B\left(\frac{\partial C}{\partial y}\right)_{y=0}. \tag{18}$$

Then, the Eq. (17) can be reduced into the dimensionless form below:

$$Cf_x Re_x^{1/2} = (1+K) f''(0), \quad Nu_x Re_x^{-1/2} = -\theta'(0), \quad Sh_x Re_x^{-1/2} = -\phi'(0). \tag{19}$$

In terms of passive control condition, the Sherwood number for passive control is identically zero [23] such that

$$Sh_x Re_x^{-1/2} = \frac{Nt}{Nb}\theta'(0), \tag{20}$$

satisfying the condition in (14).

## 3 Results and discussion

To ensure accuracy in our computation, present results are compared with the published results as presented in Tables 1, 2 and 3. In Table 1, values for reduced Nusselt number for various values of Pr and $r$ are compared with the results published by Mustafa et al. [17] who employed homotopy analysis method (HAM). Table 2 shows the comparison of the numerical values for the reduced Nusselt number and the reduced Sherwood number in the absence of elasticity and stagnation parameters as obtained by Nadeem et al. [8] using Runge–Kutta–Fehlberg method. Present results for the reduced Nusselt number when Pr is varied as compared with the results by Khan and Pop [34] who used implicit finite-difference method is presented in Table 3. From these comparison tables, it

**Table 1** Comparison of the numerical values for the reduced Nusselt number when $K = 0$, $Le = 1$ and $Nb = Nt = 0$

| Pr | $r$ | $Re_x^{-1/2}Nu_x$ | |
|---|---|---|---|
| | | Mustafa et al. [17] | Present work |
| 1.0 | 0.1 | 0.602156 | 0.602157 |
| | 0.2 | 0.624467 | 0.624469 |
| | 0.5 | 0.692460 | 0.692449 |
| 1.5 | 0.1 | 0.776802 | 0.776801 |
| | 0.2 | 0.797122 | 0.797122 |
| | 0.5 | 0.864771 | 0.864794 |

**Table 2** Comparison of the numerical values for the reduced Nusselt number, and the reduced Sherwood number in the absence of elasticity and stagnation parameter when $K = r = 0$, Pr = 10, $Le = 1$, $Nb = 0.1$ and $Nt$ is varied

| $Nt$ | Nadeem et al.[8] | | Present work | |
|---|---|---|---|---|
| | $Re_x^{-1/2}Nu_x$ | $Re_x^{-1/2}Sh_x$ | $Re_x^{-1/2}Nu_x$ | $Re_x^{-1/2}Sh_x$ |
| 0.1 | 0.9524 | 2.1294 | 0.9524 | 2.1294 |
| 0.2 | 0.6932 | 2.2732 | 0.6932 | 2.2740 |
| 0.3 | 0.5201 | 2.5286 | 0.5201 | 2.5286 |
| 0.4 | 0.4026 | 2.7952 | 0.4026 | 2.7952 |
| 0.5 | 0.3211 | 3.0351 | 0.3211 | 3.0351 |

**Table 3** Comparison of results for the reduced Nusselt number $-\theta'(0)$ for $Le = 1$, $Nb = Nt = K = 0$, $r = 1$ and Pr is varied

| Pr | $Re_x^{-1/2}Nu_x$ | |
|---|---|---|
| | Khan and Pop [34] | Present work |
| 0.70 | 0.4539 | 0.4544 |
| 2.00 | 0.9113 | 0.9114 |
| 7.00 | 1.8954 | 1.8954 |
| 20.00 | 3.3539 | 3.3539 |
| 70.00 | 6.4621 | 6.4622 |

can be verified that all present results are in good agreement with existing studies.

Analysis has been made to see the influence of various emerging parameters such as stagnation parameter $r$, elasticity parameter $K$, Lewis number $Le$, slip parameter $\alpha$, Brownian motion parameter $Nb$ and thermophoresis parameter $Nt$ in both active and passive control environments. The results of this analysis are presented in Figs. 2, 3, 4, 5, 6, 7, 8, 9, 10 and 11. Moreover, the flow streamlines and isotherms are sketched in Fig. 12. On the other hand, the numerical values of reduced skin friction coefficient, $Re_x^{1/2}C_f$, reduced Nusselt number, $Re_x^{1/2}Nu_x$ and reduced Sherwood number, $Re_x^{1/2}Sh_x$ for different values of $K$, $r$, $\alpha$, $Le$, $Nb$ and $Nt$ are also listed in Tables 4 and 5 for both active and passive controls on mass transfer.

The effects of stagnation parameter $r$ to the flow are depicted in Fig. 2. The stagnation parameter tends to increase the distributions of velocity and nanoparticle volume fraction for passive control while opposite behaviors are observed for the temperature and active controlled nanoparticle volume fraction profiles. It is also found that the presence of

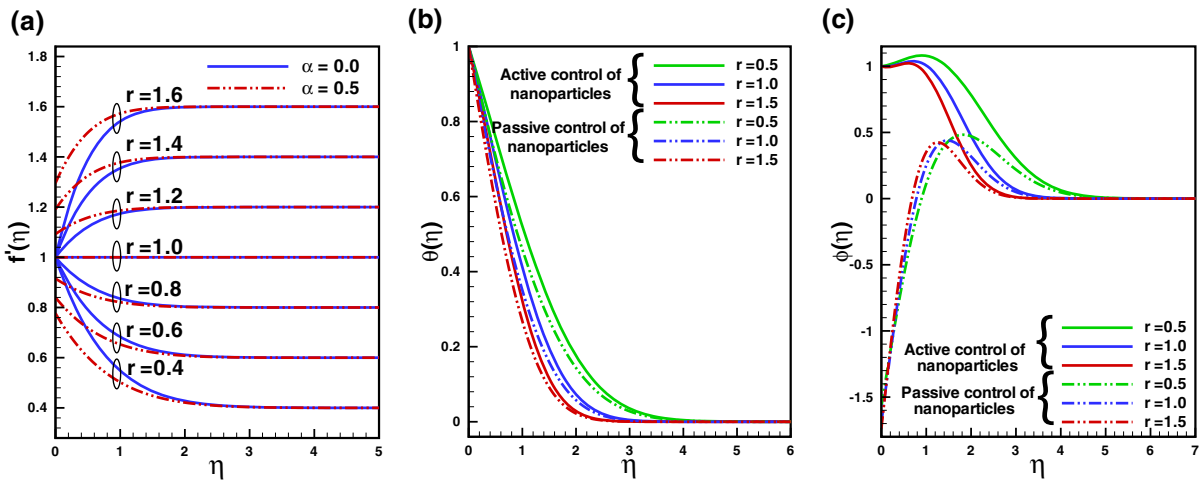


**Fig. 2** Velocity, temperature and nanoparticle volume fraction profiles for both active and passive controls when the stagnation parameter $r$ varies with $\mathrm{Pr} = 1, Le = 1, K = 0, Nb = 0.2, Nt = 0.7$ and $\alpha = 0.5$

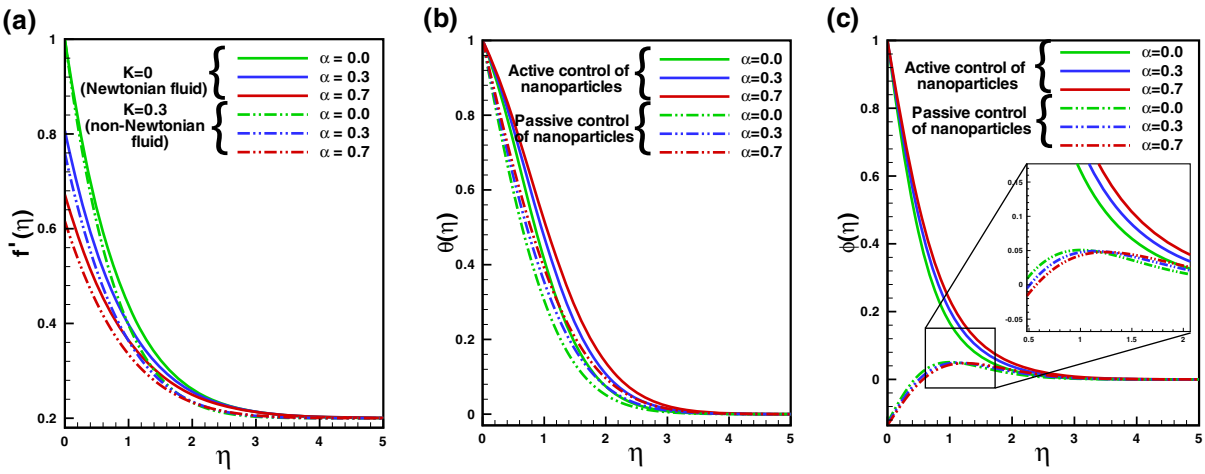


**Fig. 3** Velocity, temperature and nanoparticle volume fraction profiles for both active and passive controls when the slip parameter $\alpha$ varies with $\mathrm{Pr} = 5, Le = 1, K = 0.3, Nb = 0.5, Nt = 0.2$ and $r = 0.2$

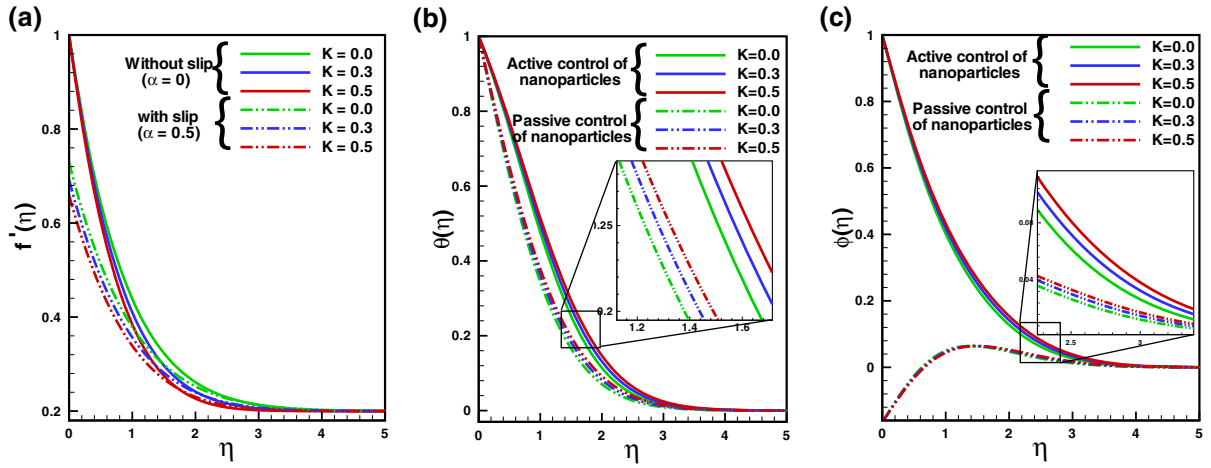


**Fig. 4** Velocity, temperature and nanoparticle volume fraction profiles for both active and passive controls when the elasticity parameter $K$ varies with $\mathrm{Pr} = 5, Le = 1, \alpha = 0.5, Nb = 0.5, Nt = 0.2$ and $r = 0.2$

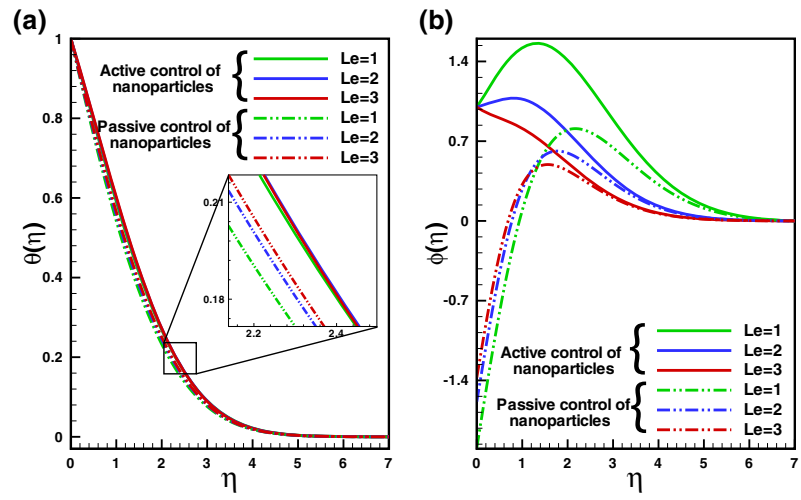


**Fig. 5** Temperature and nanoparticle volume fraction profiles for both active and passive controls when the Lewis number $Le$ varies with $\mathrm{Pr} = 5, \alpha = 1, K = 0.2, Nb = 0.1, Nt = 0.7$ and $r = 0.3$

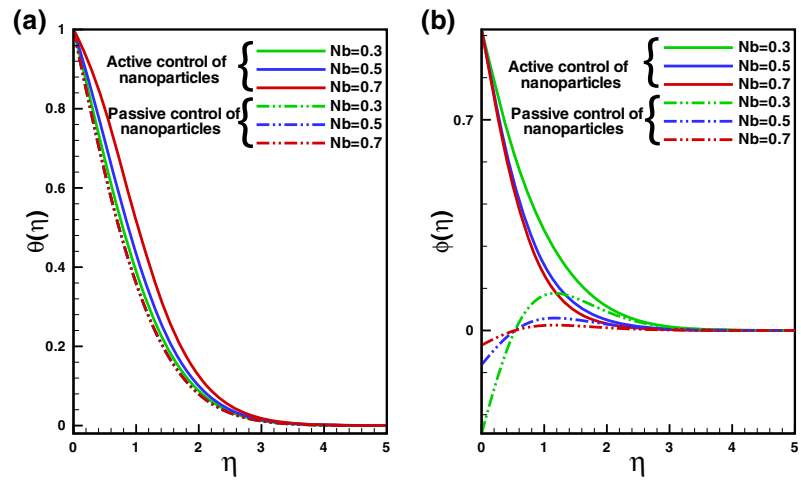


**Fig. 6** Temperature and nanoparticle volume fraction profiles for both active and passive controls when the Brownian parameter $Nb$ varies with $\mathrm{Pr} = 5, \alpha = 0.5, K = 0.3, Le = 2, Nt = 0.1$ and $r = 0.2$

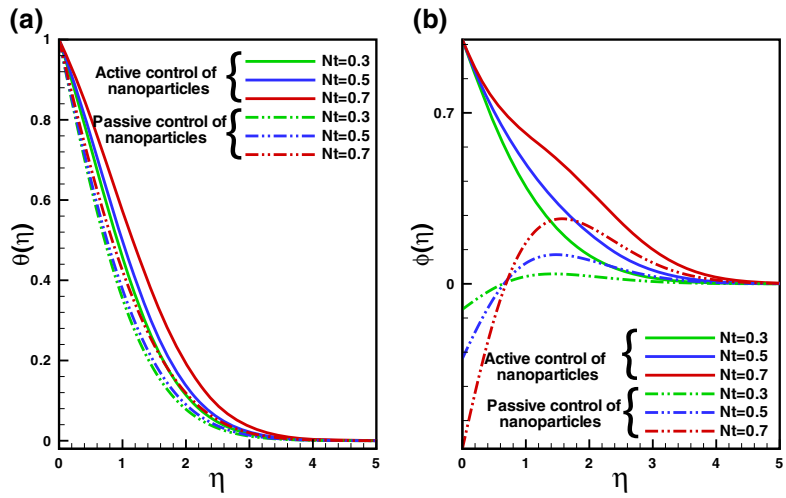


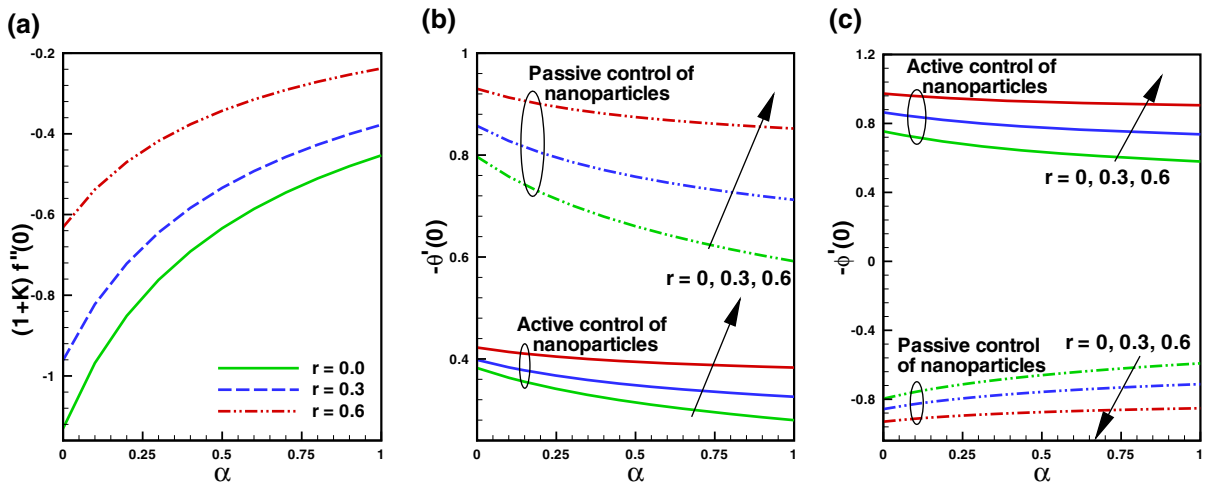


**Fig. 7** Temperature and nanoparticle volume fraction profiles for both active and passive controls when the thermophoresis parameter $Nt$ varies with $\Pr = 5, \alpha = 0.5, K = 0.3, Le = 2, Nb = 0.4$ and $r = 0.2$

**Fig. 8** Variation of reduced skin friction coefficient, reduced Nusselt number and reduced Sherwood number profiles against slip parameter, $\alpha$ when the stagnation parameter, $r$ varies with $\Pr = 5, K = 0.2, Le = 1, Nb = 0.5$ and $Nt = 0.5$

slip parameter $\alpha$ promotes acceleration for $r > 1.0$ or deceleration for $r < 1.0$ in the flow movement. Based on Figs. 3 and 4, the slip parameter $\alpha$ and elasticity parameter $K$ have the same effect on velocity and temperature. Velocity is a decreasing function while temperature is an increasing function of $\alpha$ and $K$. Increasing value of both parameter $\alpha$ and $K$ gives the effect of increasing friction in the fluid. Because of the friction, the velocity will decrease and subsequently temperature will arise as heat is being retained in the flow longer instead of being transported to the surroundings. As for the nanoparticle volume fraction in the active control, $\phi(\eta)$ will increase with increasing $\alpha$ and $K$.

From Fig. 5, it can be seen that Lewis number has an increasing effect towards temperature. However, the effect in active control is very minimal if compared relatively towards the effect in passive control. $Le$ depends on the value of thermal diffusivity and Brownian diffusion parameter. Because of the zero flux condition in passive control, value of Brownian diffusion coefficient is kept at minimum and thermal diffusivity becomes the major contributor towards value of $Le$. Hence, higher value of $Le$ means higher

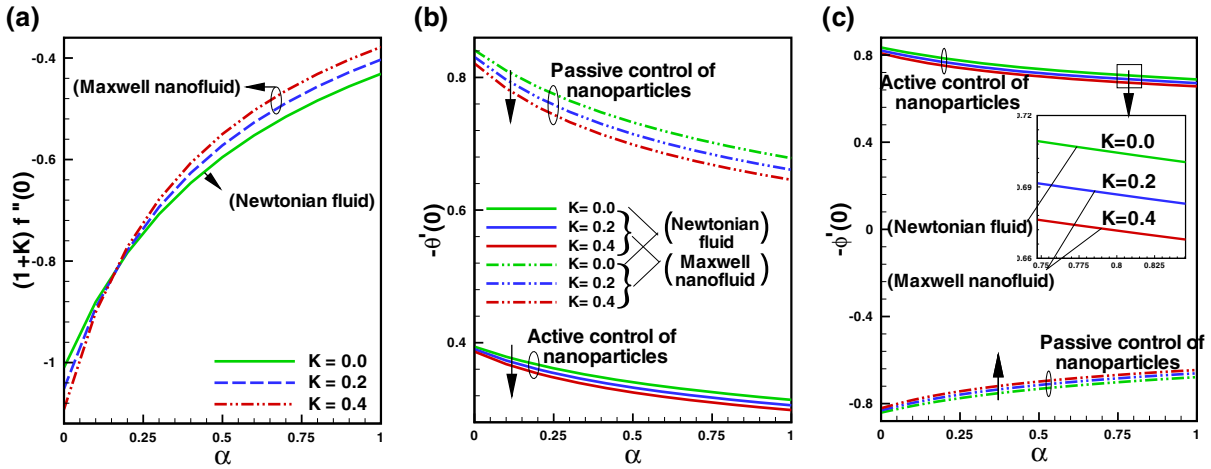


**Fig. 9** Variation of reduced skin friction coefficient, reduced Nusselt number and reduced Sherwood number profiles against slip parameter $\alpha$ when the elasticity parameter, $K$ varies with $\mathrm{Pr} = 5, r = 0.2, Le = 1, Nb = 0.5$ and $Nt = 0.5$

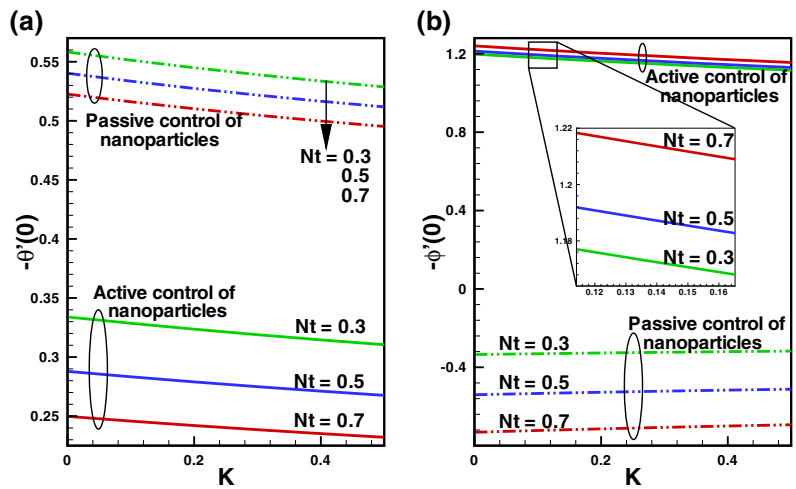


**Fig. 10** Variation of reduced Nusselt number and reduced Sherwood number profiles against elasticity parameter $K$ when the thermophoresis parameter, $Nt$ varies with $\mathrm{Pr} = 5, r = 0.2, Le = 2, Nb = 0.5$ and $\alpha = 0.5$

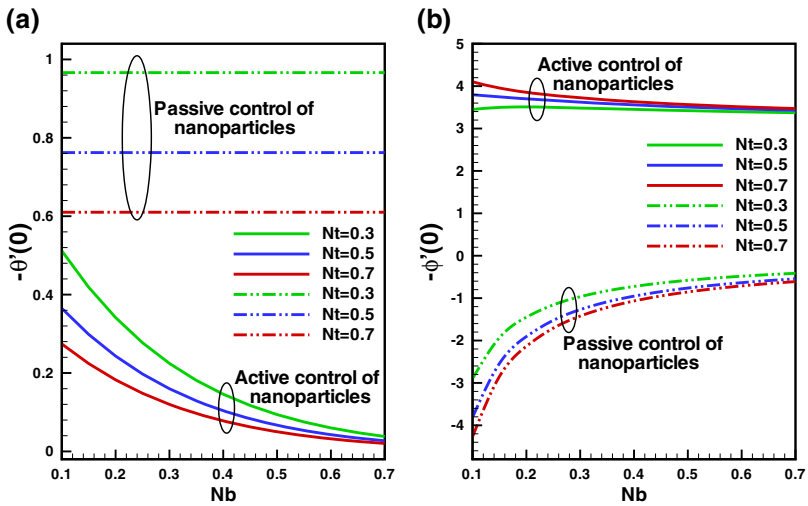


**Fig. 11** Variation of reduced Nusselt number and reduced Sherwood number profiles against Brownian parameter $Nb$ when the thermophoresis parameter, $Nt$ varies with $\mathrm{Pr} = 5, r = 0.3, Le = 5, K = 0.2$ and $\alpha = 0.5$

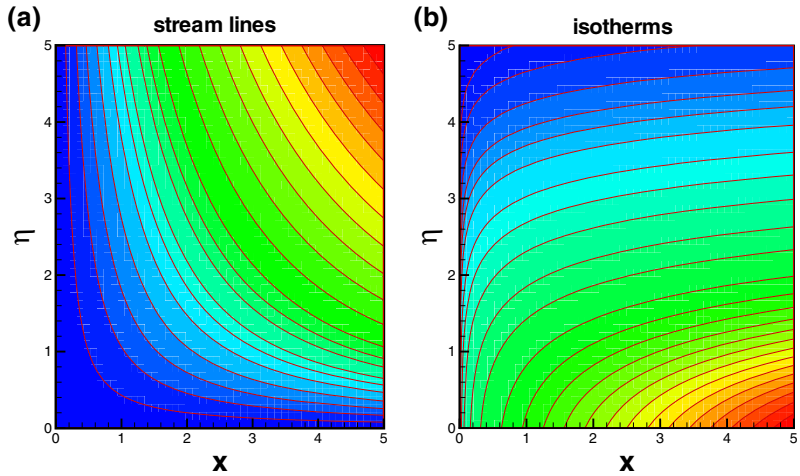


**Fig. 12** Nanofluid flow behavior: **a** stream lines and heat transfer, **b** isotherms in a whole domain

**Table 4** Values of $(1+K)f''(0), -\theta'(0)$ and $-\phi'(0)$ for both active and passive controls when $\mathrm{Pr} = 5.0, Le = 1.0$ and $Nb = Nt = 0.5$

| $K$ | $r$ | $\alpha$ | $Re_x^{-1/2}Cf_x$ | $Re_x^{-1/2}Nu_x$ | | $Re_x^{-1/2}Sh_x$ | |
|---|---|---|---|---|---|---|---|
| | | | | Active | Passive | Active | Passive |
| 0.1 | 0.2 | 0.5 | −0.57968 | 0.13044 | 1.01791 | 1.51306 | −1.01791 |
| 0.3 | | | −0.64791 | 0.12695 | 0.99024 | 1.47276 | −0.99024 |
| 0.5 | | | −0.71673 | 0.12357 | 0.95643 | 1.41977 | −0.95643 |
| 0.3 | 0.05 | | −0.70047 | 0.12489 | 0.93625 | 1.37584 | −0.93625 |
| | 0.1 | | −0.68756 | 0.12519 | 0.95067 | 1.40305 | −0.95067 |
| | 0.2 | | −0.64791 | 0.12695 | 0.99024 | 1.47276 | −0.99024 |
| | 0.2 | 0.1 | −1.06046 | 0.14572 | 1.11980 | 1.65935 | −1.11980 |
| | | 0.5 | −0.64791 | 0.12695 | 0.99024 | 1.47276 | −0.99024 |
| | | 0.9 | −0.47564 | 0.11699 | 0.92125 | 1.37304 | −0.92125 |

**Table 5** Values of $-\theta'(0)$ and $-\phi'(0)$ for both active and passive controls when $K = 0.3$, $\alpha = 0.5$, $r = 0.2$ and $\mathrm{Pr} = 5.0$

| $Le$ | $Nb$ | $Nt$ | $Re_x^{-1/2}Nu_x$ | | $Re_x^{-1/2}Sh_x$ | |
|---|---|---|---|---|---|---|
| | | | Active | Passive | Active | Passive |
| 0.1 | 0.5 | 0.5 | 0.54145 | 1.26549 | 0.01058 | −1.26549 |
| 0.5 | | | 0.19732 | 1.10965 | 0.96423 | −1.10965 |
| 1.0 | | | 0.12695 | 0.99024 | 1.47276 | −0.99024 |
| 2.0 | | | 0.08863 | 0.86291 | 2.12723 | −0.86291 |
| 1.0 | 0.3 | | 0.24901 | 0.99024 | 1.45159 | −1.65041 |
| | 0.5 | | 0.12695 | 0.99024 | 1.47276 | −0.99024 |
| | 0.7 | | 0.06136 | 0.99024 | 1.44965 | −0.70732 |
| | 0.9 | | 0.02838 | 0.99024 | 1.42375 | −0.55014 |
| | 0.5 | 0.3 | 0.17333 | 1.11641 | 1.40432 | −0.66984 |
| | | 0.5 | 0.12695 | 0.99024 | 1.47276 | −0.99024 |
| | | 0.7 | 0.09608 | 0.87336 | 1.53586 | −1.22270 |
| | | 0.9 | 0.07499 | 0.76822 | 1.59081 | −1.38280 |

thermal diffusivity which is a cause of increasing temperature. Nanoparticle volume fraction however, reacts in the opposite manner. Increasing $Le$ will decrease value of $\phi(\eta)$ in active control.

In Figs. 6 and 7, influences of nanoparticles towards temperature and nanoparticle volume fraction are observed. Increasing the value of Brownian diffusion coefficient and thermophoresis parameter will result in increasing temperature. Increasing $Nb$ means more frequent collisions where heat absorbed from the collisions causes the temperature to rise. Frequent collisions indicate that the displacements between nanoparticles are reduced hence the decrement of volume fraction occurs. When the passive mass flux condition is applied, it can be observed that $Nb$ has almost a negligible effect on temperature making the effect of $Nt$ is more significant in

temperature increment. Higher $Nt$ means a higher temperature gradient and due to the increasing temperature difference, the nanoparticles are more dispersed in order to escape to a cooler environment hence increasing the nanoparticle volume fraction in the process. In passive control, $\phi(\eta)$ shows flipping behavior but in opposite manner towards $Nb$ and $Nt$. For $Nb$, $\phi(\eta)$ increases with increasing value of $Nb$ near the wall surface but it starts to flip to decrease as it moves away farther from the wall. The same behavior of $\phi(\eta)$ can be seen in respond to increasing $r$ and $Le$ in Figs. 2c and 5b. As for $Nt$, $\phi(\eta)$ decreases near the wall before it flips to increase the same way it reacts to $\alpha$ in Fig. 3c. It can be seen in Figs. 2, 3, 4, 5, 6 and 7 that the variable $\phi(\eta)$ overshoots and attains negative values in the neighbourhood of the surface. This behavior illustrates that the nanoparticle flux at the surface is being suppressed due to passive control. Note also that the temperature for passive control model is always lower than the temperature in active control model.

Figures 8 and 9 show the influence of different values of $r$ and $K$ towards reduced skin friction coefficient $Re_x^{-1/2}Cf_x$, reduced Nusselt number $Re_x^{-1/2}Nu_x$ and reduced Sherwood number $Re_x^{-1/2}Sh_x$ with increasing value of slip velocity parameter. It is found that the reduced Nusselt number and reduced Sherwood number behave oppositely towards $\alpha$. With increasing $\alpha$, skin friction will increase while the heat flux rate will decrease. As for reduced Sherwood number, it will decrease in active control but increases in passive control. It seems that the stagnation parameter is an increasing function of $Re_x^{-1/2}Cf_x$, $Re_x^{-1/2}Nu_x$ and active control of $Re_x^{-1/2}Sh_x$. The elasticity parameter however is affected by the value of $\alpha$ in its outcome towards skin friction. When $\alpha$ is small ($<0.25$), skin friction is decreasing with increasing $K$ before it flips to increase. Meanwhile, the Nusselt number decreases when $K$ increases suggested that the heat transfer performance of Newtonian fluid when $K = 0$ in Fig. 9 is better than the non-Newtonian Maxwell fluid. Furthermore, mass flux decreases in active control but increases in passive control with increasing value of $K$. On the other hand, Figs. 10 and 11 demonstrate the effects of different values of $Nt$ towards heat and mass fluxes with increasing $K$ and $Nb$. $Re_x^{-1/2}Nu_x$ is a decreasing function of both $Nb$ (active control) and $Nt$. With increasing value of $K$ or $Nb$, $Re_x^{-1/2}Sh_x$ is an increasing function of $Nt$ in active control but a decreasing function of $Nt$ in passive control. In general, the flow shows slow behaviors in velocity and temperature which are supported by streamlines and isotherms in Fig. 12.

Tables 4 and 5 list the physical quantity values of reduced skin friction, reduced Nusselt number and reduced Sherwood number for different parameters. It is observed that the values of $Re_x^{-1/2}\ Sh_x$ in passive controls are all negative. The mass is being transferred to surroundings due to the zero mass flux condition at the surface that prevents nanoparticle deposition. Increasing values of slip parameter $\alpha$ will decrease magnitude of all physical quantities. A slight fluctuation of value on the reduced Sherwood number for active control of nanoparticles is observed when value of thermophoresis parameter $Nt$ is increasing. Meanwhile, magnitude of the reduced Nusselt number in passive control remains stagnant even though the value of Brownian parameter $Nb$ is increased. This pattern can be explained by the zero mass flux condition at the surface. It can also be suggested that in the absence of nanoparticles, there is no Brownian motion.

## 4 Concluding remarks

The problem of a two-dimensional steady viscous flow of an incompressible Maxwell fluid saturated with nanoparticles near a stagnation point over a slipped stretching surface is introduced. A hydrodynamic slip velocity is proposed as a partial expression in the general surface stretching velocity. The active control condition of nanoparticles is combined together with a realistic passive boundary condition to assume zero normal flux at the surface while taking into account the effects of both Brownian motion and thermophoresis. The model is further solved numerically using a classical shooting technique with Newton's method by utilizing MATLAB *bvp4c* function. The effects of active and passive controls of nanoparticles with emerging parameters are sketched and tabulated accordingly. The main results of the present analysis are listed below:

- Temperature distribution in passive control model is lower than the active control model.

- Both temperature and nanoparticle volume fraction settled in identical behavior for non-Newtonian elasticity and slip parameters.
- The magnitude of the reduced skin friction coefficient, Nusselt number and Sherwood number decrease as the slip parameter increases.
- The Brownian parameter has negligible effect on the reduced Nusselt number when nanoparticles are passively controlled at the surface.
- The heat transfer performance of Newtonian fluid ($K = 0$) is better than the non-Newtonian Maxwell fluid.
- The stagnation parameter promotes heat transfer performance of the flow under active and passive controls of nanoparticles.

**Acknowledgments** We thank the respected anonymous reviewer/s who contributed towards improvement of this paper. Financial support received from the Ministry of Higher Education (MOHE) Malaysia under the research Grant FRGS/1/2015/SG04/UM/02/1 (FP016-2015A) is also highly acknowledged.

## References

1. Pearson JRA, Tardy PMJ (2002) Models for flow on non-Newtonian and complex fluids through porous media. J Non-Newton Fluid Mech 102:447–473
2. Xu H, Liao SJ, Pop I (2006) Series solution of unsteady boundary layer flows of non-Newtonian fluids neat a forward stagnation point. J Non-Newton Fluid Mech 139:31–43
3. Schowalter WR (1960) The application of boundary-layer theory to power-law pseudoplastic fluids: similar solutions. AICHE J 6:24–28
4. Acrivos A, Shah MJ, Petersen EE (1960) Momentum and heat transfer in laminar boundary layer flows of non-Newtonian fluids past external surfaces. AICHE J 6:312–318
5. Shehzad SA, Alsaedi A, Hayat T (2013) Hydromagnetic steady flow of Maxwell fluid over a bidirectional stretching surface with prescribed surface temperature and prescribed surface heat flux. PLoS One 8(7):e68139. doi:10.1371/journal.pone.0068139
6. Awais M, Hayat T, Alsaedi A, Asghar S (2014) Time-dependent three-dimensional boundary layer flow of a Maxwell fluid. Comput Fluids 91:21–27
7. Abbasbandy S, Naz R, Hayat T, Alsaedi A (2014) Numerical and analytical solutions for Falkner–Skan flow of MHD Maxwell fluid. Appl Math Comput 242:569–575
8. Nadeem S, Haq RU, Khan ZH (2014) Numerical study of MHD boundary layer flow of a Maxwell fluid past a stretching sheet in the presence of nanoparticles. J Taiwan Inst Chem Eng 45:121–126
9. Ramesh GK, Gireesha BJ (2014) Influence of heat source/sink on a Maxwell fluid over a stretching surface with convective boundary condition in the presence of nanoparticles. Ain Shams Eng J 5(3):991–998
10. Hussain T, Hussain S, Hayat T (2016) Impact of double stratification and magnetic field in mixed convective radiative flow of Maxwell nanofluid. J Mol Liq 220:870–878
11. Khan N, Mahmood T, Sajid M, Hashmi MS (2016) Heat and mass transfer on MHD mixed convection axisymmetric chemically reactive flow of Maxwell fluid driven by exothermal and isothermal stretching disks. Int J Heat Mass Transf 92:1090–1105
12. Hayat T, Awais M, Qasim M, Hendi AA (2011) Effects of mass transfer on the stagnation point flow of an upper-convected Maxwell (UCM) fluid. Int J Heat Mass Transf 54:3777–3782
13. Ramesh GK, Gireesha BJ, Bagewadi CS (2012) MHD flow of a dusty fluid near the stagnation point over a permeable stretching sheet with non-uniform source/sink. Int J Heat Mass Transf 55:4900–4907
14. Ramesh GK, Gireesha BJ, Bagewadi CS (2014) Stagnation point flow of a MHD dusty fluid towards a stretching sheet with radiation. Afrika Matematika 25(1):237–249
15. Mustafa I, Javed T, Ghaffari A (2016) Heat transfer in MHD stagnation point flow of a ferrofluid over a stretchable rotating disk. J Mol Liq 219:526–532
16. Hayat T, Khan MI, Farooq M, Yasmeen T (2016) Stagnation point flow with Cattaneo–Christov heat flux and homogeneous-heterogeneous reactions. J Mol Liq 220:49–55
17. Mustafa M, Hayat T, Pop I, Asghar S, Obaidat S (2011) Stagnation-point flow of a nanofluid towards a stretching sheet. Int J Heat Mass Transf 54:5588–5594
18. Bachok N, Ishak A, Pop I (2012) The boundary layers of an unsteady stagnation-point flow in a nanofluid. Int J Heat Mass Transf 55:6499–6505
19. Alsaedi A, Awais M, Hayat T (2012) Effects of heat generation/absorption on stagnation point flow of nanofluid over a surface with convective boundary conditions. Commun Nonlinear Sci Numer Simul 17:4210–4223
20. Noor NFM, Haq RU, Nadeem S, Hashim I (2015) Mixed convection stagnation flow of a micropolar nanofluid along a vertically stretching surface with slip effects. Meccanica. doi:10.1007/s11012-015-0145-9
21. Ramesh GK, Gireesha BJ, Hayat T, Alsaedi A (2016) Stagnation point flow of Maxwell fluid towards a permeable surface in the presence of nanoparticles. Alex Eng J. doi:10.1016/j.aej.2016.02.007
22. Nield DA, Kuznetsov AV (2009) The Cheng–Minkowycz problem for natural convective boundary-layer flow in a porous medium saturated by a nanofluid. Int J Heat Mass Transf 52:5792–5795
23. Kuznetsov AV, Nield DA (2013) The Cheng–Minkowycz problem for natural convective boundary-layer flow in a porous medium saturated by a nanofluid: a revised model. Int J Heat Mass Transf 65:682–685
24. Nield DA, Kuznetsov AV (2014) The onset of convection in a horizontal nanofluid layer of finite depth: a revised model. Int J Heat Mass Transf 77:915–918
25. Kuznetsov AV, Nield DA (2014) Natural convective boundary-layer flow of a nanofluid past a vertical plate: a revised model. Int J Therm Sci 77:126–129

26. Nield DA, Kuznetsov AV (2014) Thermal instability in a porous medium layer saturated by a nanofluid: a revised model. Int J Heat Mass Transf 68:211–214
27. Rahman MM, Rosca AV, Pop I (2014) Boundary layer flow of a nanofluid past a permeable exponentially shrinking/stretching surface with second order slip using Buongiorno's model. Int J Therm Sci 77:1133–1143
28. Mustafa M, Khan JA, Hayat T, Alsaedi A (2015) Boundary layer flow of nanofluid over a nonlinearly stretching sheet with convective boundary condition. IEEE Trans Nanotechnol 14(1):159–168
29. Ul Haq R, Nadeem S, Khan ZH, Akbar NS (2015) Thermal radiation and slip effects on MHD stagnation point flow of nanofluid over a stretching sheet. Phys E 65:17–23
30. Zaimi K, Ishak A, Pop I (2011) Flow past a permeable stretching/shrinking sheet in a nanofluid using two-phase model. PLoS One 9(11):e111743. doi:10.1371/journal.pone.0111743
31. Dhanai R, Rana P, Kumar L (2015) Multiple solutions of MHD boundary layer flow and heat transfer behavior of nanofluids induced by a power-law stretching/shrinking permeable sheet with viscous dissipation. Powder Technol 273:62–70
32. Sadeghy K, Hajibeygim H, Taghavi S-M (2006) Stagnation-point flow of upper-convected Maxwell fluids. Int J Nonlinear Mech 41:1242–1247
33. Buongiorno J (2006) Convective transport in nanofluids. Trans ASME 128:240–250
34. Khan WA, Pop I (2010) Boundary-layer flow of a nanofluid past a stretching sheet. Int J Heat Mass Transf 53:2477–2483